Visualization of two transfer RNAs trapped in transit during elongation factor G-mediated translocation

David J. F. Ramrath[a,1,2], Laura Lancaster[b,1], Thiemo Sprink[a], Thorsten Mielke[a,c], Justus Loerke[a], Harry F. Noller[b,3], and Christian M. T. Spahn[a,3]

[a]Institut für Medizinische Physik und Biophysik, Charité-Universitätsmedizin Berlin, 10117-Berlin, Germany; [b]Department of Molecular, Cell and Developmental Biology, Center for Molecular Biology of RNA, University of California, Santa Cruz, CA 95064; and [c]UltraStrukturNetzwerk, Max Planck Institute for Molecular Genetics, 14195 Berlin, Germany

Contributed by Harry F. Noller, November 4, 2013 (sent for review August 22, 2013)

During protein synthesis, coupled translocation of messenger RNAs (mRNA) and transfer RNAs (tRNA) through the ribosome takes place following formation of each peptide bond. The reaction is facilitated by large-scale conformational changes within the ribosomal complex and catalyzed by elongtion factor G (EF-G). Previous structural analysis of the interaction of EF-G with the ribosome used either model complexes containing no tRNA or only a single tRNA, or complexes where EF-G was directly bound to ribosomes in the posttranslocational state. Here, we present a multiparticle cryo-EM reconstruction of a translocation intermediate containing two tRNAs trapped in transit, bound in chimeric intra-subunit ap/P and pe/E hybrid states. The downstream ap/P-tRNA is contacted by domain IV of EF-G and P-site elements within the 30S subunit body, whereas the upstream pe/E-tRNA maintains tight interactions with P-site elements of the swiveled 30S head. Remarkably, a tight compaction of the tRNA pair can be seen in this state. The translocational intermediate presented here represents a previously missing link in understanding the mechanism of translocation, revealing that the ribosome uses two distinct molecular ratchets, involving both intra- and intersubunit rotational movements, to drive the synchronous movement of tRNAs and mRNA.

ratcheting | chimeric hybrid state | ribosome dynamics | translocation mechanism | fusidic acid

During protein synthesis the ribosome iteratively incorporates new amino acids delivered by aminoacylated transfer RNAs (tRNA) into the growing polypeptide chain in a manner specified by the codons in a messenger RNAs (mRNA). This elongation cycle is controlled by the two translocational GTPases elongation factors (EF)-Tu and EF-G. Following EF-Tu–dependent delivery of aminoacyl-tRNA to the A site and peptide bond formation, the ribosome adopts a pretranslocational state containing a peptidyl A-site tRNA and a deacylated P-site tRNA. In the subsequent translocation reaction, the interplay between the ribosome and elongation factor EF-G shifts the tRNAs from the A and P sites to the P and E sites, respectively. In each of these binding sites a tRNA contacts both ribosomal subunits and interacts with the 30S and 50S subunits via its anticodon-stem loop (ASL) and acceptor arm, respectively (1). Partial tRNA movement can occur before the EF-G–dependent translocation step, involving spontaneous and reversible movement of the tRNA acceptor arms relative to the large ribosomal subunit, which leads to a shift from classic A/A and P/P binding states into intersubunit A/P and P/E hybrid states (where the first and second letters indicate tRNA contacts on the small and large subunits, respectively) (2–4).

A remarkable feature of translocation is the precise coupling of movement of the tRNAs together with the bound mRNA (designated as the $tRNA_2$•mRNA module), so that the mRNA advances by exactly one codon on the ribosome. Translocation is associated with large-scale conformational changes within the ribosomal complex, which includes rotation and back-rotation between the two subunits (during which the small subunit rotates counterclockwise and clockwise relative to the large subunit, viewing the ribosome from the solvent side of the small subunit) (5–7), and an additional forward and reverse swiveling movement of the 30S head (an autonomous domain of the 30S subunit, which can rotate around an axis roughly orthogonal to the axis of intersubunit rotation) (6, 8–13). Structural studies have suggested that intersubunit rotation within the pretranslocational complex is coupled to tRNA hybrid state formation (14–18). EF-G–dependent movement of the tRNAs and mRNA on the 30S subunit then occurs during reversal of the intersubunit rotation (6, 7). Moreover, multiparticle cryo-EM and X-ray crystallography studies suggest that movement of the tRNAs relative to the 30S subunit occurs via additional intermediate tRNA binding states, which are formed upon the back rotation of the 30S-body/platform and a large swiveling movement of the 30S head (6, 10). One of the first implications of swiveling of the 30S subunit head came from the studies of Schuwirth et al. (19), who observed a constriction of 13 Å between head and body of the 30S subunit that would block passage of tRNA between the P and E sites. These authors suggested that rotation of the 30S head would allow movement of the tRNA ASL, and could correspond to an unlocking event during translocation. Although swiveling of the

Significance

One of the most critical and complex steps of the protein synthesis elongation cycle is the coupled translocation of messenger (m)RNA and the A- and P-site transfer (t)RNAs through the ribosome, catalyzed by the elongation factor EF-G. This step involves large-scale molecular movements in the ribosome, including rotational movements of the body and head of the 30S subunit. Previously, structures have been obtained for trapped intermediates containing a single tRNA. Here, we report the cryo-EM structure of an intermediate trapped with both tRNAs. This structure represents a previously missing link in understanding the mechanism of translocation, revealing that the ribosome uses two distinct molecular ratchets, involving both intra- and intersubunit rotational movements, to drive the synchronous movement of tRNAs and mRNA.

Author contributions: D.J.F.R., L.L., H.F.N., and C.M.T.S. designed research; D.J.F.R., L.L., T.S., T.M. and J.L. performed research; L.L. contributed new reagents/analytic tools; D.J.F.R., L.L., H.F.N. and C.M.T.S. analyzed data; and D.J.F.R., L.L., H.F.N. and C.M.T.S. wrote the paper.

The authors declare no conflict of interest.

Data deposition: The data reported in this paper have been deposited in the EMDB database, www.ebi.ac.uk/pdbe/emdb/ (accession no. EMDB-5775), and the Protein Data Bank, www.ebi.ac.uk/pdbe/ (accession nos. 3j5n and 3j5o).

[1]D.J.F.R. and L.L. contributed equally to this work.

[2]Present address: Department of Biology, Institute of Molecular Biology and Biophysics, Eidgenössiche Technische Hochschule Zürich, 8093 Zürich, Switzerland.

[3]To whom correspondence may be addressed. E-mail: harry@nuvolari.ucsc.edu or christian.spahn@charite.de.

This article contains supporting information online at www.pnas.org/lookup/suppl/doi:10.1073/pnas.1320387110/-/DCSupplemental.

small subunit head has been observed in different ribosomal complexes with bound EF-G (or eEF2) (6, 8–13) or with bound tRNAs (18), it has not been observed directly in the context of an authentic translocation complex containing EF-G together with two tRNAs. Previous structural analysis of translocation used model complexes where EF-G was directly bound to either vacant ribosomes, to ribosomal complexes with one tRNA, or to complexes in the posttranslocational state (5, 6, 8, 10–13, 20–22). The present study describes a cryo-EM reconstruction more closely resembling an authentic translocation intermediate, in which EF-G•GTP was bound to a canonical pretranslocational ribosomal complex containing two tRNAs and mRNA, and stalled during the translocation reaction by the antibiotic fusidic acid (FA). The resulting sample was analyzed by means of multiparticle cryo-EM (23). The classification yielded only a single major population of 70S•EF-G•GDP•FA particles trapped in an intermediate state of the translocation reaction. In contrast to all previously described 70S•EF-G structures (5, 6, 10–13, 20–22), the resulting reconstruction directly visualizes two tRNAs bound to the ribosome in two different chimeric intrasubunit hybrid states. The data presented here show how reciprocal conformational changes within the ribosome coordinate the synchronous movement of the mRNA and bound tRNA pair.

Results

Sample Preparation and Multiparticle Classification. To analyze the mechanism of translocation, EF-G, GTP, and the antibiotic FA were incubated with *Escherichia coli* 70S ribosomes in the pretranslocational state carrying $tRNA^{fMet}$ and $Val\text{-}tRNA^{Val}$ in the P and A sites, respectively. FA specifically traps EF-G upon ribosome binding and GTP hydrolysis as it prevents complete conversion from the GTP to the GDP conformation, which is required for release of EF-G•GDP from the ribosome (6, 10, 22). The resulting sample was subjected to multiparticle classification to solve the problem of potential conformational heterogeneity within a prepared cryo-EM specimen, which can be caused by substoichiometric complex formation (23). However, the multiparticle classification of the cryo-EM dataset yielded only a single population of 279,309 70S•EF-G•GDP•FA particle images, which were used for a final cryo-EM reconstruction giving a resolution of 6.8 Å (Fig. 1 and Fig. S1). The resulting cryo-EM map shows the complex of a 70S ribosome together with EF-G bound to the factor-binding site, mRNA, and two tRNAs (Fig. 1). At this subnanometer resolution the reconstruction displays clearly visible secondary structural features, such as rod-shaped α-helical elements. This finding provided the basis for generating pseudoatomic models based on 3D coordinates of ribosomal (11), mRNA (10), tRNA (10, 22), and EF-G (11) X-ray structures.

Overall Conformation of the Ribosome. Although the composition of our specimen, which contains EF-G•GDP•FA and two tRNAs, is similar to that of the posttranslocational 70S•EF-G•GDP•FA complex, which was used for X-ray crystallography (22), remarkable large-scale differences can be observed by comparing the ribosomal conformations of the two complexes. Foremost among these structural differences is the conformation of the 30S ribosomal subunit and its orientation relative to the 50S subunit. In contrast to the X-ray structure of the posttranslocational 70S•EF-G•GDP•FA complex in a classic unrotated and unswiveled ribosomal state (22), the 30S head domain of the present complex is swiveled by ∼18°, whereas the body/platform domain has undergone a moderate rotation of ∼2.5° (Fig. 1*C*). These movements cause a displacement of peripheral elements of the 30S head over distances of up to ∼36 Å compared with a ribosome in the unrotated state (22) (Fig. 1*C*). The conformation of the present complex bears overall similarity to recently described 70S•EF-G complexes designated as translocation intermediate (TI^{POST}) (6) or GDPNP-II (10) characterized by an intermediate (∼5°) body/platform rotation and large (∼18°) head swivel. However, the latter complexes contained only a single tRNA (6, 10), whereas the present complex contains two tRNAs, more closely resembling an authentic translocation intermediate (TI^{POST}). In this view, the TI^{POST} state is adopted after formation of the preceding TI^{PRE} state, which was observed with a single bound tRNA (6, 12, 13). This TI^{PRE} to TI^{POST} transition would include a back-rotation of the body/platform region from ∼7–9° to ∼2.5° and an additional swiveling movement of the 30S head domain from ∼5–7.5° to ∼18°. In agreement with the X-ray structures of 70S•EF-G complexes (10), the present structure also shows that the swiveling movement of the 30S head is accompanied by a lateral movement of the tip of Helix H38 (also called the A-site finger) and leads to formation of a new intersubunit contact formed between S19 and the tip of the A-site finger (*SI Results and Discussion* and Fig. S2).

Structural Characterization of the tRNA Binding Sites. The observed structural changes of the ribosome have a unique influence on the interactions between the ribosome and bound tRNAs. In each of the three classic binding states a tRNA interacts with a specific set of rRNA and ribosomal protein residues, which are distributed between both ribosomal subunits (1). In the trapped intermediate structure described here, the CCA acceptor ends of the tRNAs are fully translocated from the P and A sites to the E and P sites,

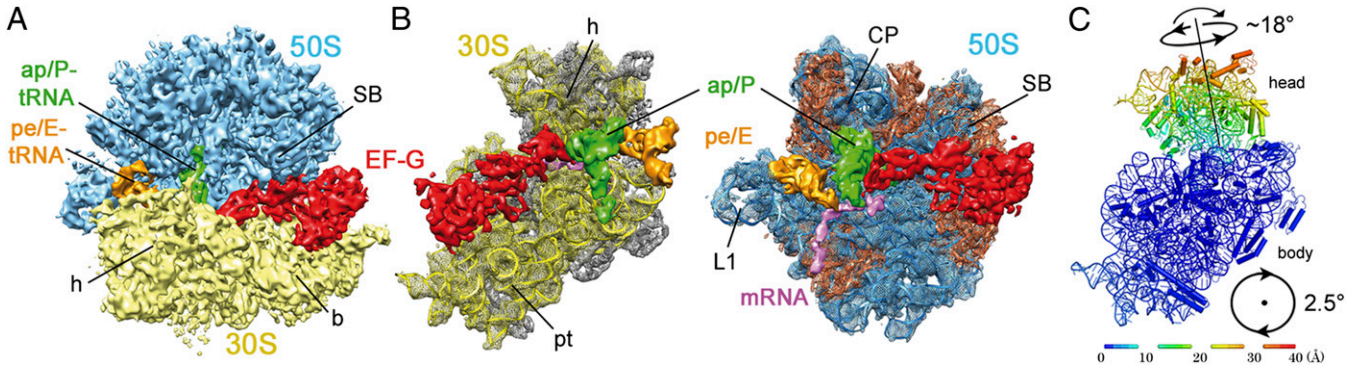

Fig. 1. Overview of the canonical TI^{POST} complex. (*A* and *B*) Cryo-EM density of the ligands ap/P- and pe/E-tRNAs (green and orange), mRNA (magenta), and EF-G (red) in surface representation within the 70S complex [50S (blue) and 30S (yellow)] (*A*) or with a mesh representation of both subunits together with docked models of the 30S [16S (yellow) and S-proteins (gray)] and 50S [23S and 5S (blue) and L-proteins (orange)] (*B*). (*C*) View from the intersubunit space onto the 30S subunit in the presented authentic TI^{POST} complex. Elements are colored according to their structural displacement compared with the classic conformation (30) upon a common 50S alignment.

respectively, on the 50S subunit (Fig. 1*B*). However, the tRNA ASLs have moved to an intermediate state of translocation relative to the 30S subunit. Interactions between the ASLs of the Val-tRNA^{Val} and tRNA^{fMet} and the A- and P-site elements of the 30S body are disrupted and replaced by contacts with 16S rRNA P- and E-site residues A790 and U788/A695, respectively (Fig. S3). At the same time, the ASL of tRNA^{fMet} maintains its characteristic P-site contacts with A1229, G1338, and A1339 within the 30S head, as it moves to follow the large ∼18° swiveling movement of the 30S head (Fig. S3). The latter movement results in a chimeric hybrid binding state (the pe/E state; where p and e indicate contact between the ASL and the P site of the 30S head and E site of the 30S body/platform; and E indicates contact of the acceptor end with the 50S E site) in which the ASL of tRNA^{fMet} is held between the P site of the 30S head and the E site of the 30S body, whereas its CCA acceptor end is bound to the 50S E site, as observed in previous 70S•EF-G complexes containing a single tRNA (6, 10). Meanwhile, contacts between the ASL of the A-site Val-tRNA^{Val} and the A-site elements of the 30S body are disrupted, as the ASL had moved during TI^{POST} state formation. This process results in formation of an additional chimeric hybrid state (the ap/P state) in which the ASL is positioned between the A site of the 30S head and the P site of the 30S body, whereas its acceptor end is bound to the 50S P site (Fig. S3). This observed network of ribosome–tRNA interactions is distinct from the posttranslocational 70S•EF-G•GDP•FA complex in which the tRNAs are bound in their classic P/P and E/E binding states (22), and to rotated pretranslocational ribosome complexes with tRNAs bound in intersubunit A/P and P/E hybrid states (14–18) (Fig. S3). Therefore, the Val-tRNA^{Val} and tRNA^{fMet} bound in the complex presented here occupy a pair of tRNA binding states that can be understood as chimeric intrasubunit ap/P and pe/E hybrid states, which is consistent with related single-molecule studies (24). Although the pe/E binding state is similar to that observed previously for trapped ribosome•EF-G intermediate complexes containing a single tRNA (6, 10), the ap/P tRNA represents a previously unobserved binding state whose functional role was predicted by a recently suggested model for canonical translocation (6).

Within the present FA-stalled intermediate, the tRNA$_2$•mRNA module has already moved relative to the 50S subunit and the 30S body/platform domain, in agreement with a toe-print signal, which indicated full mRNA-translocation for a similar FA-trapped ribosomal complex (25). This observation is consistent with the results of presteady-state kinetics experiments, which showed that GTP hydrolysis by EF-G precedes movement of the tRNA$_2$•mRNA module (26). Movement then occurs independent of and parallel to the release of P$_i$ from the ribosome-bound EF-G•GDP•P$_i$ complex. However, as shown here, translocation is not completed in this FA-stalled state because the 30S head still maintains its characteristic pretranslocational A and P site contacts with the ap/P- and pe/E-tRNAs (Fig. S3). The kinetic model of Savelsbergh et al. (26) does not account for the occurrence of multiple steps of mRNA and tRNA movement. In light of the important role of 30S head rotation, it seems likely that this is a consequence of basing this model on a fluorescence quenching assay to detect mRNA movement. As discussed elsewhere (9), quenching may occur when the mRNA is moved into contact with the head or body of the 30S subunit, or alternatively when the 30S subunit head or body rotates into contact with the mRNA during their respective reverse rotations; these different possibilities render the interpretation of the quenching results ambiguous. Thus, the quenching assay may not report on the final steps of translocation.

EF-G Contacts the ap/P-tRNA, mRNA, and the 30S Head. The reconstruction of the present complex displays well-defined cryo-EM density for EF-G, which binds to the factor-binding site and places its domain IV into the ribosomal A site (Fig. 2). In this

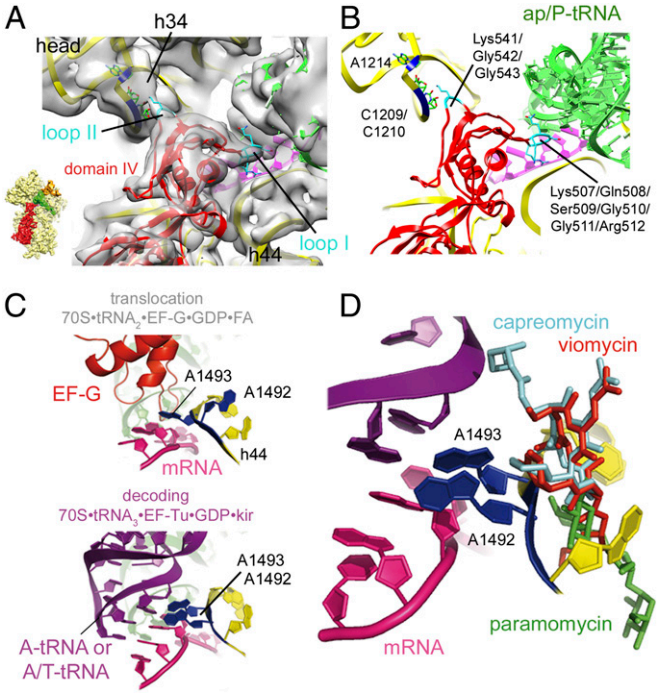

Fig. 2. Contacts of EF-G domain IV. (*A*) Cryo-EM density of the presented TI^{POST} complex shown as transparent gray surface together with docked models of the 30S, mRNA, ap/P-tRNA, and EF-G (colored as in Fig. 1) in the indicated view (*Left*). (*B*) Cartoon representation of the canonical TI^{POST} complex highlighting the interactions between loop I and loop II within EF-G domain IV and the minor grooves of the mRNA codon–tRNA anticodon helix, as well as h34, respectively. (*C*) Cartoon representation of the A1492 and A1493 (blue) within h44 (yellow) in their tentative positions during translocation (suggested by the present authentic TI^{POST}) (*Upper*) and upon domain closure during decoding (observed in a 70S•tRNA$_3$•EF-Tu•GDP•kir complex) (43) (*Lower*). (*D*) Cartoon representation of A1492 and A1493 as shown in *C, Lower*, together with the antibiotics paramomycin (green) (32), viomycin (red), and capreomycin (cyan) (31).

position, domain IV establishes contacts with the ap/P-tRNA, mRNA and h34 of 16S rRNA in the swiveled head (Fig. 2). Thus, the structure unifies separate structural observations coming from other 70S•EF-G complexes, in which either the domain IV–codon-anticodon interaction (22) or the domain IV–h34 contact were observed (6, 10). Interestingly, there are certain similarities in comparing the two contacts between EF-G and the two RNA helices, h34 and the mRNA codon–ap/P-tRNA anticodon helix (codon-anticodon helix). In each case, one of two protruding loops at the tip of domain IV (loop I or loop II) intercalates into the minor groove of the codon-anticodon helix or h34 of 16S rRNA, respectively. Remarkably, at the apical tips of both loops two neighboring glycine residues, which are 100% conserved among bacteria [Gly510/Gly511 and Gly542/Gly543 (*E. coli* nomenclature) for loop I and loop II, respectively] facilitate the tight turns required for their intercalation into the RNA minor grooves (Fig. 2*B*). Including all EF-G residues within 5 Å of mRNA and the ap/P-tRNA, the loop I region of EF-G buries a surface area of ∼1,000 Å^2; in contrast, the loop II region buries an area of only ∼390 Å^2 (Fig. 2). Accordingly, the loop I–codon-anticodon helix interaction may act as a robust "doorstop" to prevent back-slippage of the ap/P-tRNA and mRNA, whereas the less extensive loop II–h34 contact may help to stabilize the orientation of the 30S head. The latter interaction can explain why binding of EF-G leads to transient protection of h34 against chemical modification during the translocation reaction (27). In this regard the present structure reveals an important function of EF-G and explains the overall shape of its

domain IV. Like a hand with two protruding fingers, domain IV uses loop I and loop II to establish simultaneous protein–RNA minor groove interactions with the codon-anticodon RNA triplet, as well as with h34. These data reveal how EF-G stabilizes the synchronous movement of the ap/P-tRNA anticodon, its corresponding mRNA codon, and the associated swiveling of the 30S head in the course of translocation. In addition, in agreement with observations coming from a high-resolution X-ray structure of a 70S•EF-G complex (13) and related data from a 80S•eEF2 complexes at intermediate resolution (28), the present data suggest that EF-G might trigger conformational changes within the 30S decoding center (Fig. 2 *C* and *D* and Fig. S4). These changes may include reorientation of A1492 and lead to destabilization of its interaction with the minor groove of the codon-anticodon helix. Such an interpretation would be consistent with the results of presteady-state kinetics studies (29) and may explain the inhibitory effects of the antibiotics paromomycin and viomycin, which reduce the rate of translocation by about 160- and >10,000-fold, respectively (30). Both antibiotics bind around h44 and stabilize the flipped-out positions of A1492 and A1493 (31, 32) (Fig. 2*D*). In particular, the presence of viomycin prevents such a proposed reorientation, as it would sterically clash with a reoriented A1492 (31) (Fig. 2*D*). This suggested mechanism would be consistent with kinetic and FRET studies, both of which describe translocation intermediates that can be stalled by viomycin (33, 34). Factor-induced rearrangements within the small subunit-decoding center residues were also observed during eukaryotic translation initiation (35). In the context of these structural data (13, 28, 29, 33–35) the small subunit-decoding center may be seen as a general pivotal element of the ribosome, whose flexibility is precisely controlled by external factors to coordinate several steps during different phases of translation.

tRNA Compaction. Comparison of the present tRNAs in their intrasubunit ap/P and pe/E hybrid states with tRNAs in classic A, P, and E sites using a 50S alignment (36) reveals a gap between the ASLs of the pe/E- and E-site tRNAs, placing the pe/E-tRNA ASL 4 Å closer to the P site (Fig. 3). The cognate E-site tRNA was selected for the present comparison because it directly interacts with the corresponding mRNA E site codon and creates at least one base pair of the codon-anticodon triplet (36, 37). However, the observed pe/E-tRNA superimposes closely on the pe*/E-tRNA bound to 70S•EF-G complex in an overall similar conformation (GDPNP-II) (10). Accordingly, the detected 4 Å gap indicates that the movement of the tRNA from the P to the E site is not fully completed during the FA-stalled TI^{POST} state formation. Apparently, a further movement of the tRNA must occur during the final step of translocation: that is, the release of EF-G•GDP and reverse rotation of the 30S subunit head. Such an interpretation would be compatible with the reported presteady-state kinetic model (26). Although the used biochemical system does not provide a resolution to describe such small-scale tRNA movements, the derived model indicates that translocation is completed by rearrangements within EF-G and the ribosome (26). Furthermore, we observe compaction of the tRNA pair during the translocation reaction. TI^{POST} formation moves the P-site tRNA ASL by about 20 Å from its classic position into the pe/E state (measuring the distance between their respective nucleotides at position 31). In contrast, the A-site tRNA moves by about 32 Å into the ap/P state and is thus pushed against the pe/E-tRNA ASL, presumably stabilized by its interaction with EF-G domain IV. Thus, the two tRNA ASLs move closer together, as indicated by the 20 Å distance between their apical base pairs and may even allow tRNA–tRNA contact in this state (Fig. 3*A*). In contrast, much larger equivalent distances of 32.5 Å and 24 Å are observed between adjacent tRNAs occupying classic A and P or P and E sites, respectively (Fig. 3*D*).

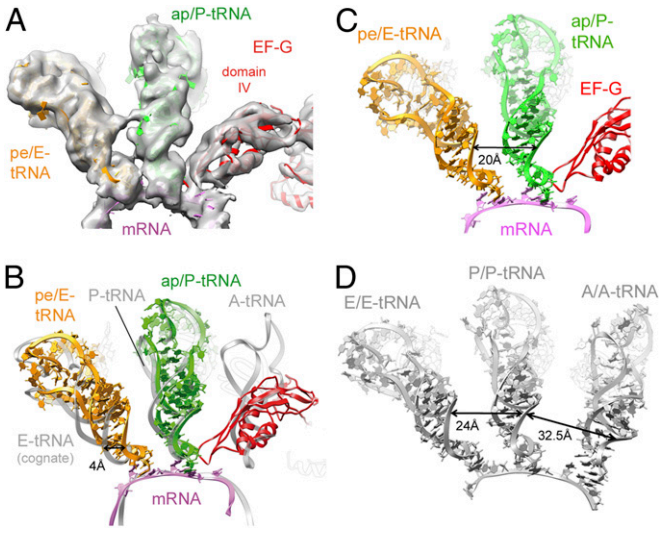

Fig. 3. Ligand positions within the authentic TI^{POST}complex. (*A*) Cryo-EM density for the ligands within the presented authentic TI^{POST} complex in a transparent surface representation together with docked models of EF-G (red), ap/P-tRNA (green), pe/E-tRNA (orange), and mRNA (magenta). (*B*) Superimposition of the ligands (as shown in *A*) together with tRNAs bound to classic A, P, and E sites (transparent gray) (23) upon a 50S alignment. (*C* and *D*) Ribbon representation of the ribosomal ligands within the present authentic TI^{POST} complex (*C*), and an unrotated ribosomal complex with classic A, P, and E-tRNAs (23) (*D*). Highlighted are the distances between the last base pair within ASL of bound tRNAs.

Ribosome–tRNA Interactions. Interestingly, the present reconstruction shows very tight interactions between the 30S subunit and the two tRNAs that involve canonical P-site contacts in both cases. In the 30S platform, A790 contacts the "downstream" ap/P-tRNA, whereas around the 30S head G1338/A1339 contacts the "upstream" pe/E-tRNA (Fig. 4 *A* and *B*). Thus, the P-site interactions are partitioned between the two tRNAs in their observed transit states. Furthermore, the reconstruction suggests that both tRNAs maintain tight interactions with their corresponding mRNA codons (Fig. 4*C*). Close interaction between the pe/E-tRNA anticodon and mRNA codon created by three base pairs was also observed in the overall similar 70S•EF-G (GDPNP-II) structure with a single bound pe*/E-tRNA (10). Notably, our data suggest that consecutive codon–anticodon interactions are maintained in both chimeric ap/P and pe/E tRNA binding sites (Fig. 4*C*). The anticodon loop positions of the pe/E-and P-site tRNA closely overlap using a 30S-head alignment (Fig. 4*D*), suggesting that the interactions with G1338/A1339 provide the major contribution in shaping the binding pocket of the pe/E-tRNA anticodon loop.

Discussion

Coordinated Movement of tRNAs and mRNA. During the translocation reaction, the ribosome—together with its bound ligands—must ensure stringent coupling of the movement of the two tRNAs together with their associated mRNA so that the mRNA advances by exactly one codon. The structure of the present authentic TI^{POST} complex reveals two tRNAs bound in chimeric intrasubunit ap/P and pe/E binding states trapped in an intermediate state of translocation. In these positions, both tRNAs appear to interact with their mRNA codons. We note that at the present resolution, it cannot be concluded with absolute certainty that the mRNA has moved along with the tRNAs and that the codon/anticodon densities represent canonical pairs. Nevertheless, a toe-printing study of an equivalent complex indicated that mRNA movement had already occurred in the FA-stalled state (25), although our structure

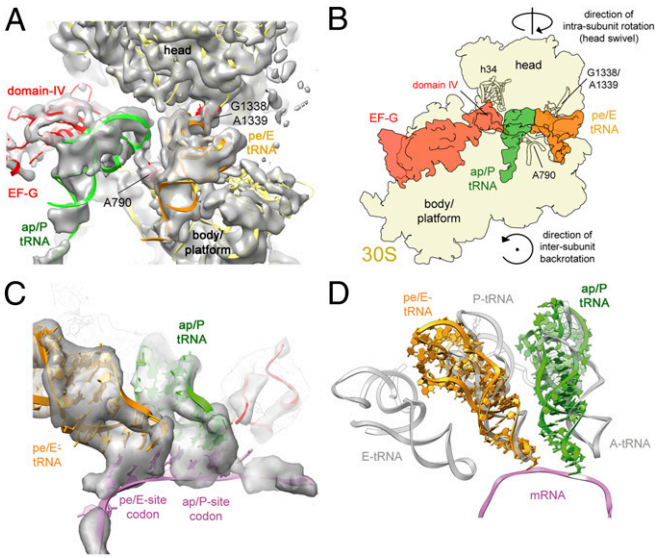

Fig. 4. Ribosome–tRNA interactions. (*A*) Cryo-EM density for the 30S and ligands within the presented authentic TI^{POST} complex in a transparent gray surface representation together with docked models of the 30S (yellow), ap/P-tRNA (green), pe/E-tRNA (orange), and EF-G (red). (*B*) Schematic of the 30S subunit and bound ligands [EF-G (red), ap/P-tRNA (green) and pe/E-tRNA (orange)] from the presented authentic TI^{POST}. (*C*) Cryo-EM density of the ligands within the presented authentic TI^{POST} (transparent gray surface) together with docked models of EF-G, pe/E-tRNA, ap/P-tRNA, and mRNA (colored as in *A*). (*D*) Superimposition of the ligands from the present authentic TI^{POST} complex with either tRNAs in classic A, P, and E-site (23) (transparent gray) upon a 30S head alignment.

demonstrates that translocation is not yet completed. Maintaining consecutive codon–anticodon interactions during translocation could explain how both tRNAs contribute to avoid a frameshift event.

In addition, the present structure suggests how coupling of the movement of mRNA and tRNAs is promoted by the ribosome and EF-G during TI^{POST} formation. Around the ribosomal A site, synchronous movement of the mRNA codon and tRNA anticodon is mediated via interactions with a loop (loop I) that protrudes from the tip of domain IV of EF-G and inserts into the minor groove of the codon-anticodon helix (Figs. 2 and 4). A second loop (loop II) protruding from the tip of domain IV inserts into the minor groove of h34 of 16S rRNA in the head of the 30S subunit. In this way, domain IV of EF-G interconnects the downstream ap/P-tRNA and its A-site codon with the head of the ribosomal 30S subunit. If these interactions form before movement of the mRNA and tRNA ASLs, they would link the swiveling of the 30S head to movement of the $tRNA_2$•mRNA module. Around the ribosomal E site, the 16S rRNA residues G1338 and A1339 of the 30S head appear to maintain a tight grip on the upstream pe/E-tRNA, leading to a precise positioning of the tRNA ASL (Fig. 4). Movement of the downstream ap/P-tRNA toward the pe/E-tRNA ASL then results in compaction of the tRNA pair (Fig. 3).

In agreement with our recent suggested model (6), the present work suggests that the ASLs of both tRNAs are moved from the A/P and P/E states within a rotated pretranslocated complex to the chimeric ap/P and pe/E states of the TI^{POST}. This movement is accompanied by a swiveling movement of the 30S head from ~5–7.5° to ~18° and the back rotation of the 30S body/platform from presumably ~7–9° to the observed ~2.5°. Key interactions for synchronization of head-swiveling with tRNA and mRNA movement appear to be G1338 and A1339 for the pe/E-tRNA and coupling of ap/P-tRNA and mRNA to h34 by domain IV of EF-G (Figs. 2 and 4). After the back rotation of the 30S body/platform and the EF-G–stabilized compaction of the tRNA pair, the ap/P-tRNA creates a tight interaction with the 16S rRNA residue A790 within the 30S body/platform (Fig. 4). Because of this interaction, the ap/P-tRNA and the 30S body/platform stabilize each other in the respective observed positions. This observation complements related findings coming from the X-ray structure of a 70S•EF-G complex (GDPNP-II) in an overall similar conformation (10). This X-ray structure showed intercalation of the universally conserved 16S rRNA bases C1397 and A1503 in the body of the 30S subunit between mRNA bases. By defining the first nucleotide of the P-site codon as +1, C1397 intercalates between positions +9 and +10 mRNA nucleotides and A1503 between −1 and −2; it was suggested that they could potentially act as molecular pawls to prevent slippage of the mRNA during reverse rotation of the 30S head. The ap/P-tRNA–A790 interaction may stabilize a specific conformation of the 30S body/platform after its back rotation from ~7–9° to ~2.5°. The EF-G–stabilized compaction of the tRNA pair may be coupled via the ap/P-tRNA–A790 contact to the positioning of the 30S body/platform, including the bases C1397 and A1503. By this mechanism, the positions of both intercalated bases (C1397 and A1503) relative to the mRNA would be stabilized after tRNA compaction and associated movement of the mRNA.

This sequence of events may also explain the process of programmed +1 frameshifts, which were shown to occur in vitro (38) and in vivo (39) and suppressed by frameshift-suppressor tRNAs that contain an extra base in their anticodon loops. Structural studies have demonstrated that such tRNAs use anticodons loops with a special architecture and may span a four-base mRNA quadruplet around the ribosomal A site, but still allow the formation of the regular minor groove geometry required for decoding (40). Accordingly, during translocation such a quadruplet codon may passively follow the frameshift-suppressor tRNA codon into the ribosomal ap/P-site stabilized by loop I within EF-G domain IV. The +1 frameshift can then be manifested by intercalation of C1397 between +10 and +11 and of A1503 between −1 and −2.

These structural observations may also rationalize why two tRNAs (or minimally, a P-site tRNA and an ASL bound to the A site) are required for effective translocation (41). The intrasubunit chimeric pe/E state state can be occupied by a single-bound tRNA as visualized by cryo-EM (6) and X-ray crystallography (10). If such a single-bound pe/E-tRNA maintained its tight interactions with the 30S head during the final steps of translocation (i.e., reverse rotation of the head and release of EF-G•GDP), it would be repositioned in the classic 30S P site rather than being moved into the posttranslocated 30S E-site in the absence of a second tRNA. However, reaccess to the classic 30S P site would be prevented by steric clash with an ap/P-tRNA, which is stabilized by interactions with A790 and possibly EF-G domain-IV.

Conclusion

The structure presented here represents a previously undescribed visualization of a translocation intermediate containing two tRNAs. This visualization suggests that EF-G stabilizes the swiveling movement of the 30S head, the synchronous movement of mRNA and tRNA through the A site, and compaction of the tRNA pair. The ribosome can be described as a bimodular molecular ratchet that can undergo intrasubunit (30S head swivel) and intersubunit rotations. The canonical P-site contacts (A790 within the body and G1338/A1339 within the head) may act as molecular pawls to couple these reciprocal rotations to the coordinated and synchronous movement of tRNAs and mRNA.

Materials and Methods

Pretranslocational ribosomal complexes were prepared carrying an mRNA, a $tRNA^{fMet}$, and a Val-$tRNA^{Val}$ in the P and A site, respectively. Such pretranslocational complexes were incubated with EF-G in the presence of

FA and GTP. The obtained complex was flash-frozen in liquid ethane. Subsequently, cryo-EM data were collected using a Tecnai G^2 Polara Microscope (FEI) and scanned using a D8200 Primscan drum scanner (Heidelberger Druckmaschinen). Digitized data were processed using multiparticle classification protocols (23) implemented with SPIDER (42). Further details are presented in *SI Materials and Methods*.

ACKNOWLEDGMENTS. We thank J. Buerger for his assistance during the cryo-EM data collection, Lucas Horan for the double-mutant ribosome construct, and D. Ermolenko for critical discussions. This work was supported by a grant from the Federation of European Biochemical Societies Long-Term Fellowship (to D.J.F.R.); National Institutes of Health Grants GM-17129 and GM-59140 (to H.F.N.); and Deutsche Forschungsgemeinschaft Grants FOR 1805 and SFB 740 (to C.M.T.S.).

1. Yusupov MM, et al. (2001) Crystal structure of the ribosome at 5.5 A resolution. *Science* 292(5518):883–896.
2. Moazed D, Noller HF (1989) Intermediate states in the movement of transfer RNA in the ribosome. *Nature* 342(6246):142–148.
3. Blanchard SC, Kim HD, Gonzalez RL, Jr., Puglisi JD, Chu S (2004) tRNA dynamics on the ribosome during translation. *Proc Natl Acad Sci USA* 101(35):12893–12898.
4. Munro JB, Altman RB, O'Connor N, Blanchard SC (2007) Identification of two distinct hybrid state intermediates on the ribosome. *Mol Cell* 25(4):505–517.
5. Frank J, Agrawal RK (2000) A ratchet-like inter-subunit reorganization of the ribosome during translocation. *Nature* 406(6793):318–322.
6. Ratje AH, et al. (2010) Head swivel on the ribosome facilitates translocation by means of intra-subunit tRNA hybrid sites. *Nature* 468(7324):713–716.
7. Ermolenko DN, Noller HF (2011) mRNA translocation occurs during the second step of ribosomal intersubunit rotation. *Nat Struct Mol Biol* 18(4):457–462.
8. Spahn CM, et al. (2004) Domain movements of elongation factor eEF2 and the eukaryotic 80S ribosome facilitate tRNA translocation. *EMBO J* 23(5):1008–1019.
9. Guo Z, Noller HF (2012) Rotation of the head of the 30S ribosomal subunit during mRNA translocation. *Proc Natl Acad Sci USA* 109(50):20391–20394.
10. Zhou J, Lancaster L, Donohue JP, Noller HF (2013) Crystal structures of EF-G–ribosome complexes trapped in intermediate states of translocation. *Science* 340(6140): 1236086.
11. Pulk A, Cate JH (2013) Control of ribosomal subunit rotation by elongation factor G. *Science* 340(6140):1235970.
12. Tourigny DS, Fernández IS, Kelley AC, Ramakrishnan V (2013) Elongation factor G bound to the ribosome in an intermediate state of translocation. *Science* 340(6140): 1235490.
13. Chen Y, Feng S, Kumar V, Ero R, Gao YG (2013) Structure of EF-G–ribosome complex in a pretranslocation state. *Nat Struct Mol Biol* 20(9):1077–1084.
14. Agirrezabala X, et al. (2008) Visualization of the hybrid state of tRNA binding promoted by spontaneous ratcheting of the ribosome. *Mol Cell* 32(2):190–197.
15. Julián P, et al. (2008) Structure of ratcheted ribosomes with tRNAs in hybrid states. *Proc Natl Acad Sci USA* 105(44):16924–16927.
16. Fischer N, Konevega AL, Wintermeyer W, Rodnina MV, Stark H (2010) Ribosome dynamics and tRNA movement by time-resolved electron cryomicroscopy. *Nature* 466(7304):329–333.
17. Budkevich T, et al. (2011) Structure and dynamics of the mammalian ribosomal pretranslocation complex. *Mol Cell* 44(2):214–224.
18. Agirrezabala X, et al. (2012) Structural characterization of mRNA-tRNA translocation intermediates. *Proc Natl Acad Sci USA* 109(16):6094–6099.
19. Schuwirth BS, et al. (2005) Structures of the bacterial ribosome at 3.5 A resolution. *Science* 310(5749):827–834.
20. Valle M, et al. (2003) Locking and unlocking of ribosomal motions. *Cell* 114(1): 123–134.
21. Connell SR, et al. (2007) Structural basis for interaction of the ribosome with the switch regions of GTP-bound elongation factors. *Mol Cell* 25(5):751–764.
22. Gao YG, et al. (2009) The structure of the ribosome with elongation factor G trapped in the posttranslocational state. *Science* 326(5953):694–699.
23. Loerke J, Giesebrecht J, Spahn CM (2010) Multiparticle cryo-EM of ribosomes. *Methods Enzymol* 483:161–177.
24. Wang L, Altman RB, Blanchard SC (2011) Insights into the molecular determinants of EF-G catalyzed translocation. *RNA* 17(12):2189–2200.
25. Spiegel PC, Ermolenko DN, Noller HF (2007) Elongation factor G stabilizes the hybrid-state conformation of the 70S ribosome. *RNA* 13(9):1473–1482.
26. Savelsbergh A, et al. (2003) An elongation factor G-induced ribosome rearrangement precedes tRNA-mRNA translocation. *Mol Cell* 11(6):1517–1523.
27. Matassova AB, Rodnina MV, Wintermeyer W (2001) Elongation factor G-induced structural change in helix 34 of 16S rRNA related to translocation on the ribosome. *RNA* 7(12):1879–1885.
28. Taylor DJ, et al. (2007) Structures of modified eEF2 80S ribosome complexes reveal the role of GTP hydrolysis in translocation. *EMBO J* 26(9):2421–2431.
29. Khade PK, Joseph S (2011) Messenger RNA interactions in the decoding center control the rate of translocation. *Nat Struct Mol Biol* 18(11):1300–1302.
30. Peske F, Savelsbergh A, Katunin VI, Rodnina MV, Wintermeyer W (2004) Conformational changes of the small ribosomal subunit during elongation factor G-dependent tRNA-mRNA translocation. *J Mol Biol* 343(5):1183–1194.
31. Stanley RE, Blaha G, Grodzicki RL, Strickler MD, Steitz TA (2010) The structures of the anti-tuberculosis antibiotics viomycin and capreomycin bound to the 70S ribosome. *Nat Struct Mol Biol* 17(3):289–293.
32. Ogle JM, Murphy FV, Tarry MJ, Ramakrishnan V (2002) Selection of tRNA by the ribosome requires a transition from an open to a closed form. *Cell* 111(5):721–732.
33. Pan D, Kirillov SV, Cooperman BS (2007) Kinetically competent intermediates in the translocation step of protein synthesis. *Mol Cell* 25(4):519–529.
34. Nguyen B, Ticu C, Wilson KS (2010) Intramolecular movements in EF-G, trapped at different stages in its GTP hydrolytic cycle, probed by FRET. *J Mol Biol* 397(5): 1245–1260.
35. Weisser M, Voigts-Hoffmann F, Rabl J, Leibundgut M, Ban N (2013) The crystal structure of the eukaryotic 40S ribosomal subunit in complex with eIF1 and eIF1A. *Nat Struct Mol Biol* 20(8):1015–1017.
36. Jenner LB, Demeshkina N, Yusupova G, Yusupov M (2010) Structural aspects of messenger RNA reading frame maintenance by the ribosome. *Nat Struct Mol Biol* 17(5):555–560.
37. Feng S, Chen Y, Gao YG (2013) Crystal structure of 70S ribosome with both cognate tRNAs in the E and P sites representing an authentic elongation complex. *PLoS ONE* 8(3):e58829.
38. Hohsaka T, Taira H, Fukushima M, Sisido M (2001) Effect of single base insertion into anticodon loop of frameshift suppressor tRNA. *Nucleic Acids Res Suppl* (1):189–190.
39. Pande S, Vimaladithan A, Zhao H, Farabaugh PJ (1995) Pulling the ribosome out of frame by +1 at a programmed frameshift site by cognate binding of aminoacyl-tRNA. *Mol Cell Biol* 15(1):298–304.
40. Dunham CM, et al. (2007) Structures of tRNAs with an expanded anticodon loop in the decoding center of the 30S ribosomal subunit. *RNA* 13(6):817–823.
41. Joseph S, Noller HF (1998) EF-G–catalyzed translocation of anticodon stem-loop analogs of transfer RNA in the ribosome. *EMBO J* 17(12):3478–3483.
42. Frank J, et al. (1996) SPIDER and WEB: Processing and visualization of images in 3D electron microscopy and related fields. *J Struct Biol* 116(1):190–199.
43. Schmeing TM, et al. (2009) The crystal structure of the ribosome bound to EF-Tu and aminoacyl-tRNA. *Science* 326(5953):688–694.

Supporting Information

Ramrath et al. 10.1073/pnas.1320387110

SI Materials and Methods

Biochemical Methods. *Escherichia coli* elongation factor (EF)-G, cloned into pET21b (Novagen), was expressed in strain BLR (DE3) by growing cells at 37 °C in LB plus ampicillin (100 μg/mL) to an A^{550} of 0.8, followed by induction with isopropyl-β-D-thiogalactopyranoside (1-mM final concentration) and continued growth for 3 h. Cells were lysed in 25 mM Tris·Cl (pH 7.5), 40 mM NH_4Cl, and 5 mM βME, then centrifuged at 30,000 × *g* for 20 min in a JA20 rotor. The supernatent containing soluble EF-G (35 mL) was mixed with 6 g of DEAE-cellulose (Whatman DE-52) pre-equilibrated in lysis buffer. After washing the resin with 1 L of lysis buffer, proteins were eluted with 25 mM Tris·Cl (pH 7.5), 300 mM NH_4Cl, 5 mM βME, then dialyzed against buffer A [25 mM Tris·Cl (pH 7.5), 60 mM NH_4Cl, 5 mM βME]. EF-G was further purified by FPLC chromatography using a 6-mL Resource-Q anion-exchange column (Pharmacia) and eluted with a 200-mL salt gradient from 60 to 300 mM NH_4Cl in buffer A. For further purification using a 10 mL Toyopearl Butyl-650S (BTP) column, fractions containing EF-G were pooled and one-third volume of 4 M ammonium sulfate (AS) was added to bring the final concentration to 1 M AS. EF-G was eluted from the BTP column with a 200-mL gradient of 1 M to 0 AS in buffer A. EF-G–containing fractions were pooled, dialyzed into buffer A, concentrated to less than 300 μL using an Amicon Ultra 15 (Millipore; 10,000 molecular-weight cutoff) concentrator, then additionally purified on a 24 mL Superdex 75 gel filtration column (Pharmacia) preequilibrated in buffer A. EF–G–containing aliquots were flash-frozen in liquid nitrogen and stored at −80 °C.

Aminoacylation of transfer RNA (tRNA) (Sigma) was carried out as described previously (1). Messenger RNA (mRNA) MV27 (GGCAAGGAGGUAAAAAUGGUAAAAAAA) (IDT) codes for Met (AUG) in the P site and Val (GUA) in the A site.

In the course of the described work we also analyzed 70S-EF-G complexes carrying an intersubunit disulfide cross-link. The aim was to analyze the influence of such a cross-link onto the conformational modes of the ribosomal complex. Ribosomes containing an intersubunit disulphide cross-link between ribosomal proteins S6 and L2 were purified as described previously (2).

Ribosomes were heat-activated and the intersubunit disulphide cross-link was reduced by incubating in buffer B [80 mM KHepes (pH 7.5), 75 mM NH_4Cl, 20 mM $MgCl_2$] with the addition of 100 mM βME, at 42 °C for 10 min. Next, 15 pmol of ribosomes, 30 pmol of mRNA MV27, and 30 pmol of deacylated $tRNA^{fMet}$ were incubated at 37 °C for 15 min in buffer B in a total volume of 14 μL. Then, 20 pmol of Val-$tRNA^{Val}$ (1.1 μL) were added and the reaction was incubated an additional 30 min at 37 °C; 60 pmol of EF-G, 0.4 mM fusidic acid (FA) and 1 mM GTP were incubated for 5 min at 37 °C in buffer B in a total volume of 15 μL, before adding to the ribosome complex (total volume 30 μL), and incubating at room temperature for 20 min in 80 mM KHepes (pH 7.5), 75 mM NH_4Cl, 10 mM $MgCl_2$, and 6 mM βME. Five-microliter aliquots were flash-frozen in liquid nitrogen and stored at −80 °C.

Cryo-EM and Image Processing. Ribosomal complexes were diluted to a final concentration of 30 nM and subsequently flash-frozen onto Quantifoil grids using a Vitrobot (FEI) device. Micrographs were recorded on film (Kodak-SO163) under low-dose conditions (20 $e^{-}\cdot Å^{-2}\cdot s^{-1}$) using a Tecnai G^2 Polara (FEI) cryo electron microscope operated at 300 kV and a magnification of 39,000×. Micrographs were collected at an underfocus that ranged from 2 to 5 μm and subsequently scanned using a D8200 Primscan drum scanner (Heidelberger Druckmaschinen) with a step size of 4.758 μm, corresponding to 1.26 Å on the object scale.

The contrast transfer function defocus values for the micrographs were determined using CTFind (3). Candidates for projection images of the ribosome were automatically identified using Signature (4) and subsequently screened. All steps of image processing were performed using the SPIDER software package (5). Multiparticle refinement was carried out as described previously (6). Particle images belonging to subpopulations of ribosomal particles that did not contain EF-G were selected out and not used for a further analysis. Finally 279,309 particle images derived from 308 micrographs were used to reconstruct the 70S•$tRNA_2$•mRNA•EF-G•GDP•FA complex. At the final rounds of the refinement, high-spatial frequencies were enhanced using the power spectrum derived from an atomic model of a 70S ribosomal complex (7) as reference. Subsequently the reconstructed map was low-pass filtered according to the current resolution estimate, which finally reached a value of 6.8 Å using the 0.5 Fourier shell correlation (FSC) criteria (Fig. S1).

Generation of Pseudoatomic Models. Rigid-body docking of high-resolution X-ray structures of the ribosomal 50S subunit [PDB ID code 4KIX (8)], 30S-head, and 30S-body/platform [PDB ID code 4KIY (8)] was performed using University of California at San Francisco chimera (9). A model of the pe/E-$tRNA^{fMet}$ was generated on the basis of pe/E*-$tRNA^{Met}$ [PDB ID code 4KBT (10)] crystal structure by docking the anticodon stem loop of the $tRNA^{Met}$ (nucleotides U27–A43) together with the corresponding mRNA codon, as well as the acceptor stem, TΨC- and D-loop of the pe/E*-$tRNA^{Met}$ (nucleotides C1–G26 and A44–A76). Both elements were docked individually into the observed pe/E-tRNA density and subsequently combined by allowing flexibility in the C25–G30 and C40–C48 region. Flexibility around this region of a tRNA was also observed when a tRNA adopts an A/T state (A site on 30S and EF-Tu-bound on the 50S subunit) or P/E state of binding as seen by X-ray crystallography (10, 11), as well as cryo-EM (12, 13). A model of the $tRNA^{Val}$ was generated by using a P site bound $tRNA^{fMet}$ together with the corresponding mRNA codon [PDB ID code 2WRI (14)]. To match the used experimental conditions, the sequences of the mRNA codon and tRNA anticodon were changed (i.e., a U34-A35-C36 $tRNA^{Val}$ anticodon was inserted into the docked P-$tRNA^{fMet}$, which is complementary to the used GUA mRNA codon). Both docked mRNA codons were combined and the mRNA was extended in both (3′ and 5′) directions as long as assigned cryo-EM density was visible.

SI Results and Discussion

Unique Intersubunit Bridge Between the A Site Finger, L5, and S19. The position of the swiveled head as it is observed in the present authentic TI^{POST} is stabilized by the formation of a unique intersubunit contact (Fig. S2). On the basis of docked models, the new bridge is created between protein L5 within the central protuberance, the tip of Helix-38 [also termed A-site finger (ASF)] and the ribosomal protein S19 within the swiveled head (Fig. S2*A*). The cryo-EM reconstruction displays a well-defined and continuous density between the C-terminal part of L5 (presumably around Arg-177 and Lys-178), the tip of the ASF, and a central loop of protein S19 (around Lys-27 and Lys-28) (Fig. S2*A*). These structural data reveal that the conformational changes underlying TI^{POST}-formation are also located within the large

ribosomal subunit. In comparison with the conformation of a pretranslocational ribosomal complex with classic bound tRNAs (15), the ASF is undergoing a conformational change during translocation intermediate (TI) TI^{POST}-formation, which shifts its tip over a distance of ~10 Å (Fig. S2 *B* and *C*). Movement of the ASF was also observed in parallel studies analyzing the translocation of the large tmRNA (16) and the different subconformations of a mammalian pretranslocational 80S ribosomal complex (17). However, certain differences can be observed regarding the directions and magnitudes of these movements of the dynamic ASF.

Tentative Assignment of the Configurations of A1492 and A1493 and Their Potential Role During Translocation. In addition to the described interactions between EF-G, the ap/P-tRNA, mRNA, and h34 of the swiveled 30S-head the highly conserved EF-G residues Ser589 and Glu590 (*E. coli* nomenclature) located around the N terminus of helix α-13 make a tentative contact with the adenosine base of the flipped-out A1493. This interaction was also observed in the crystal structure of the posttranslocational 70S•EF-G•GDP•FA complex (14). Similarly, the presented reconstruction of the authentic TI^{POST} indicates the presence of a gap within the cryo-EM density of h44, which corresponds to the helical position of A1493 (Fig. S4). However, the reconstruction also shows well-defined density in the close vicinity of the helical position of A1493, which corresponds to the A1492 position (Fig. S4). Both of these two rRNA residues of the 30S-decoding center are known to be flexible and different possible orientations and positions of both residues were reported by X-ray crystallography (14, 18–20). In view of the given resolution of 6.8 Å, the best apparent agreement between three different orientations and the present cryo-EM density can be observed by an orthogonal orientation of both residues (orthogonal orientation of A1492 relative to flipped-out A1493) (Fig. S4*C*). Such a configuration was also observed in the crystal structure of a 70S•EF-G complex (21). A flipped-out position for both bases, A1492 as well as A1493, was suggested by cryo-EM maps of 80S•eEF2 complexes at intermediate resolutions (22).

Presteady-state kinetic measurements revealed that during translocation an EF-G, induced ribosome rearrangement precedes the $tRNA_2$•mRNA movement and represents the rate-limiting step of the entire reaction (23). In line with this observation, more recent data revealed that the destabilization of the minor groove interactions between the A site mRNA codon and in particular A1492 lead to a significant increase in the overall rate of translocation (24). During the elongation cycle, translocation follows the delivery of an aminoacyl-tRNA (decoding) and the subsequent peptidyl transfer. In the process of decoding, both rRNA residues A1492 and A1493 adopt flipped-out positions (as shown in Fig. S4*A*) and interact with the minor groove of the codon-anticodon triplet around the A site (18, 19).

Accordingly, the suggested position of A1492 (orthogonal configuration relative to A1493) indicated by the present reconstruction of the authentic TI^{POST} (Fig. S4*C*) might correspond to the ribosomal conformation triggered by EF-G. Thus, the data suggest that an EF-G induced reorientation of A1492 is part of the rate-limiting ribosome rearrangement, which is consistent with the reported presteady-state kinetics (23, 24).

1. Lancaster L, Noller HF (2005) Involvement of 16S rRNA nucleotides G1338 and A1339 in discrimination of initiator tRNA. *Mol Cell* 20(4):623–632.
2. Horan LH, Noller HF (2007) Intersubunit movement is required for ribosomal translocation. *Proc Natl Acad Sci USA* 104(12):4881–4885.
3. Mindell JA, Grigorieff N (2003) Accurate determination of local defocus and specimen tilt in electron microscopy. *J Struct Biol* 142(3):334–347.
4. Chen JZ, Grigorieff N (2007) SIGNATURE: A single-particle selection system for molecular electron microscopy. *J Struct Biol* 157(1):168–173.
5. Frank J, et al. (1996) SPIDER and WEB: Processing and visualization of images in 3D electron microscopy and related fields. *J Struct Biol* 116(1):190–199.
6. Loerke J, Giesebrecht J, Spahn CM (2010) Multiparticle cryo-EM of ribosomes. *Methods Enzymol* 483:161–177.
7. Selmer M, et al. (2006) Structure of the 70S ribosome complexed with mRNA and tRNA. *Science* 313(5795):1935–1942.
8. Pulk A, Cate JH (2013) Control of ribosomal subunit rotation by elongation factor G. *Science* 340(6140):1235970.
9. Pettersen EF, et al. (2004) UCSF Chimera—A visualization system for exploratory research and analysis. *J Comput Chem* 25(13):1605–1612.
10. Zhou J, Lancaster L, Donohue JP, Noller HF (2013) Crystal structures of EF-G–ribosome complexes trapped in intermediate states of translocation. *Science* 340(6140):1236086.
11. Schmeing TM, et al. (2009) The crystal structure of the ribosome bound to EF-Tu and aminoacyl-tRNA. *Science* 326(5953):688–694.
12. Ratje AH, et al. (2010) Head swivel on the ribosome facilitates translocation by means of intra-subunit tRNA hybrid sites. *Nature* 468(7324):713–716.
13. Schuette JC, et al. (2009) GTPase activation of elongation factor EF-Tu by the ribosome during decoding. *EMBO J* 28(6):755–765.
14. Gao YG, et al. (2009) The structure of the ribosome with elongation factor G trapped in the posttranslocational state. *Science* 326(5953):694–699.
15. Agirrezabala X, et al. (2008) Visualization of the hybrid state of tRNA binding promoted by spontaneous ratcheting of the ribosome. *Mol Cell* 32(2):190–197.
16. Ramrath DJF, et al. (2012) The complex of tmRNA-SmpB and EF-G on translocating ribosomes. *Nature* 485(7399):526–529.
17. Budkevich T, et al. (2011) Structure and dynamics of the mammalian ribosomal pretranslocation complex. *Mol Cell* 44(2):214–224.
18. Ogle JM, et al. (2001) Recognition of cognate transfer RNA by the 30S ribosomal subunit. *Science* 292(5518):897–902.
19. Ogle JM, Murphy FV, Tarry MJ, Ramakrishnan V (2002) Selection of tRNA by the ribosome requires a transition from an open to a closed form. *Cell* 111(5):721–732.
20. Berk V, Zhang W, Pai RD, Cate JH (2006) Structural basis for mRNA and tRNA positioning on the ribosome. *Proc Natl Acad Sci USA* 103(43):15830–15834.
21. Chen Y, Feng S, Kumar V, Ero R, Gao YG (2013) Structure of EF-G–ribosome complex in a pretranslocation state. *Nat Struct Mol Biol* 20(9):1077–1084.
22. Taylor DJ, et al. (2007) Structures of modified eEF2 80S ribosome complexes reveal the role of GTP hydrolysis in translocation. *EMBO J* 26(9):2421–2431.
23. Savelsbergh A, et al. (2003) An elongation factor G-induced ribosome rearrangement precedes tRNA-mRNA translocation. *Mol Cell* 11(6):1517–1523.
24. Khade PK, Joseph S (2011) Messenger RNA interactions in the decoding center control the rate of translocation. *Nat Struct Mol Biol* 18(11):1300–1302.
25. Yusupov MM, et al. (2001) Crystal structure of the ribosome at 5.5 A resolution. *Science* 292(5518):883–896.

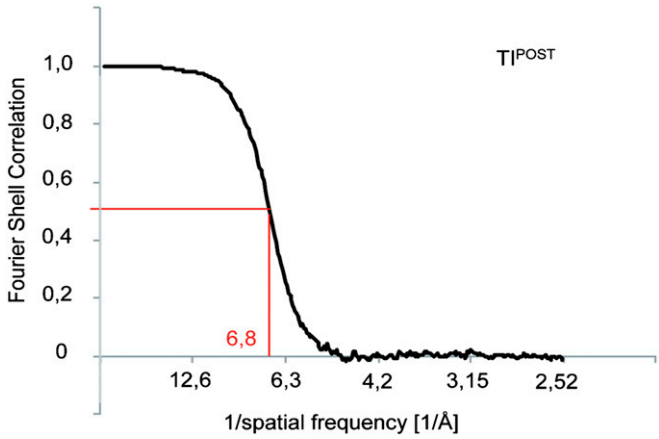

Fig. S1. Resolution curves of the authentic TI^{POST}. According to the 0.5 FSC cut-off, the resolution of the authentic TI^{POST} complex is 6.8 Å.

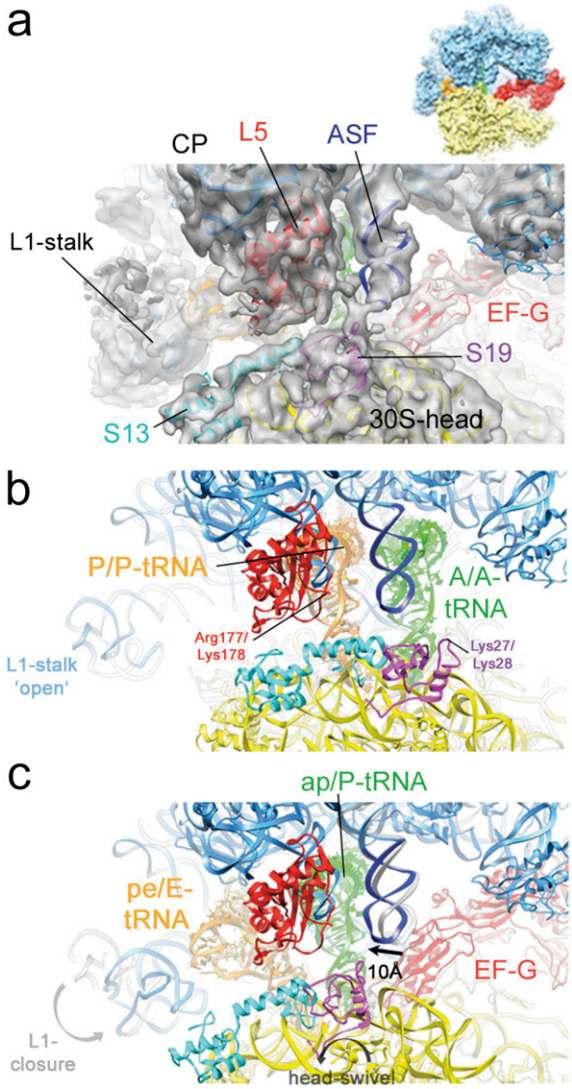

Fig. S2. Formation of a unique intersubunit bridge. (*A*) Cryo-EM density of the authentic TI^{POST} shown as gray transparent surface with docked models of the ribosome [30S (yellow), 50S (blue), S13 (cyan), S19 (magenta)], EF-G (red), and tRNAs [ap/P-tRNA (green), pe/E-tRNA (orange)]. The map displays a continuous density between L5 (red), the ASF (dark blue), and S19 (magenta). (*B*) Cartoon representation of the ribosomal conformation in the classic unrotated classic pretranslocational state (15) with an opened L1-stalk indicating the contact between the ASF and S13. (*C*) Cartoon representation of the authentic TI^{POST} indicating the structural changes of the 30S-head, ASF, and L1-stalk. The positions of L1-stalk and ASF as shown in *B* are displayed in transparent gray.

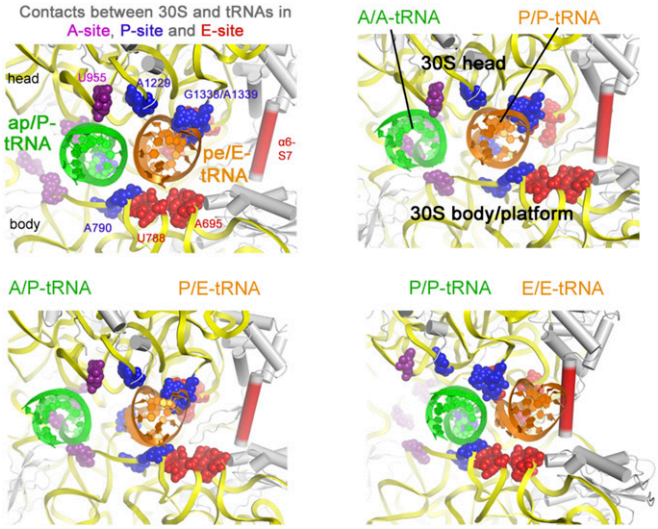

Fig. S3. Interactions of the 30S subunit and different bound tRNAs. Ribbon representation of the tRNA binding region on the 30S subunit. Residues that contact tRNAs in the A (magenta), P (blue), and E site (red) (25) are shown as spheres together with two tRNAs in chimeric intrasubunit (ap/P and pe/E), classic (A/A andP/P), intersubunit hybrid (A/P and P/E), or classic posttranslcoated (P/P and E/E) tRNA binding sites (14, 15).

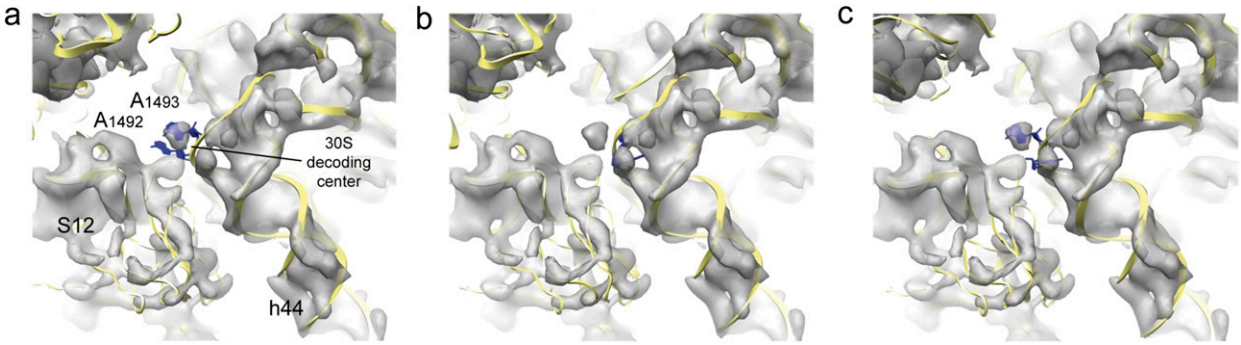

Fig. S4. Comparison of different orientations of A1492 and A1493 and the presented cryo-EM reconstruction. View from the intersubunit space onto the cryo-EM density for the 30S decoding center from the presented authentic TI^{POST} (transparent gray) together with docked models from Gao et al. (14) (*A*), Pulk and Cate (8) (*B*), and Berk et al. (20) (*C*) showing different observed orientations of A1492 relative to A1493.